

SEISMIC ISOLATED HOUSE REACTION UPON CONDITION OF THE REPEATABILITY OF EARTHQUAKES

Lapin Vladimir^{1*}, Sharipov Rashid², Aldakhov Yerkin³

¹ Kazakh Research and Design Institute of Construction and Architecture, Almaty, Republic of Kazakhstan

² Kazakh-German University, Almaty, Republic of Kazakhstan

³ Director of Seismic Resistance and Survey Center, KazRDICA JSC, Almaty, Republic of Kazakhstan

* vladimir.zuev.ro85@mail.ru

To study the seismic properties of buildings in Almaty, a special test site operates. It includes buildings with conventional strip foundations with a system of cross belts and seismic support of 2 types. The landfill buildings were previously tested under static and dynamic influences. With the use of real accelerograms of earthquakes, a forecast of the behavior of a seismically isolated house on kinematic foundations under seismic influences has been carried out. The seismic impact is represented by a set of real accelerograms of strong, mainly Californian earthquakes. The hearts depths and magnitudes correspond to possible Almaty earthquakes. Two design schemes of a seismically isolated building are considered - single-mass and 10-mass dynamic building models. It is shown that the magnitudes of displacements in the kinematic foundations (KF) level obtained by two dynamic models usually differ within 5-10%. Therefore, the calculation of seismically isolated buildings can be applied to a single-mass non-linear dynamic model. A linear regression connection was obtained between the values of acceleration at the base and displacements at the level of the foundation. For the values of acceleration according to the new "Map of seismic zoning of the Republic of Kazakhstan" were obtained the predicted values of displacement at the level of the kinematic support of the order of 8.0-11.5 cm.

Keywords: seismic isolation, accelerogram, safety, forecast, foundation, computational model, earthquake recurrence

1 INTRODUCTION

A fairly simple and effective means of reducing the risk of losses in case of possible earthquakes are seismic isolation systems of various types, which have been intensively developing over the past 30 years [1-15]. Several thousand seismically isolated objects have already been built in the world.

In JSC "KazRDICA" (Republic of Kazakhstan), studies of evaluating the effectiveness of seismic isolation systems of various types are carried out at a permanently operating special test site (Almaty). In 1989, on three built houses with the same above-foundation part (9-storey large-panel houses of the 158 series) were installed the stations of the engineering and seismometric service, but with different foundations: conventional tape with a system of cross belts, seismic kinematic and supports with fluoroplastic gaskets [12].

In [16], the behavior of seismically insulated buildings is studied during the strong Baikal earthquake on August 27, 2008 with $M_w = 6.2$. This is the strongest earthquake in the Baikal region over the past 60 years. In the city of Irkutsk, the intensity of the earthquake was 6-7 points. A survey of residents who were in seismically insulated houses during the earthquake (buildings on kinematic foundations) revealed that they did not even feel the vibrations, unlike people who are in traditional buildings. In buildings without seismic isolation systems, loose objects fell, people experienced panicky. There was no damage in the seismically isolated houses.

It should be noted that the territory of the megalopolis of the city of Almaty is the most earthquake-prone region of Central Asia, where earthquakes with a magnitude of up to 8 are possible. In 1911, the Kemin earthquake of a class of seismic disasters with a magnitude of 8.2 took place [17]. The city of Verny (now the city of Almaty) was practically destroyed by this earthquake.

Therefore, it is very important to predict the behavior of seismically insulated buildings during possible local earthquakes. The task is to predict the response of a seismically isolated building on kinematic foundations, taking into account data on the recurrence of earthquakes from the "Map of seismic zoning of the Republic of Kazakhstan", which was introduced in 2017. This task is very urgent and was not set earlier.

2 MATERIALS AND METHODS

The typical building is a large-panel residential building of the 158 series, a single-entrance block section. Building dimensions: length-17.4 m, width-12.9 m, height - 31.5 m. The building has 9 floors, each 3 m high, with an additional technical underground and a semi-walk-through attic. There are several hundred such buildings in the city of Almaty.

Let's calculate the seismically isolated building taking into account the regional features of the seismic impact for the city of Almaty - a megalopolis with a population of over 2 million people. According to the current "Map of seismic zoning of the Republic of Kazakhstan", the median values of acceleration in the city are equal with a recurrence rate of 1 time in 475 years 0.38g, and at 1 time in 2475 years - 0.73g. Here g is the gravity acceleration.

The seismic impact is represented by a set of real accelerograms of strong, mainly Californian earthquakes. The source depths of which and the magnitude values correspond to possible Almaty earthquakes.

Analysis of the results of previous experimental studies showed that since shear deformations prevail in the building, shear deformations are an acceptable design scheme [1,2,4].

Therefore, a multi-storey building appears to be a discrete console with lumped masses. The physical properties of the tiers are described by experimental nonlinear deformation diagrams.

It is convenient to describe nonlinear deformation diagrams by piecewise linear dependencies. It is known that piecewise linear deformation diagrams with an arbitrary number of linear sections allow one to approximate practically any experimental diagrams. Therefore, the deformation diagram of the KF is assumed to be nonlinear elastic, consisting of 6 linear sections, and the floor deformation diagrams are trilinear elastoplastic.

The parameters of the deformation diagram for the KF are determined from experimental data using the experimental results of previous studies.

The nine-storey building is modeled by a 10-mass nonlinear system, where the bottom mass corresponds to the basement of the building and the rest to the residential floors. For the case of a building with KF, the lower mass simulates the kinematic foundation.

Energy dissipation in the system is described by Voigt's hypothesis.

The weights of the concentrated masses of the building are taken to be the same and equal to 2700 kN.

The solution of a system of 10 nonlinear differential equations was carried out by the Runge-Kutta method using CKM MATLAB solvers with automatic selection of the integration step.

For the presentation, it is convenient to introduce the following correspondence:

Object A - large-panel building 158 series with kinematic foundations;

Object B is a large-panel building with conventional foundation.

Thus, during the study, experimental deformation diagrams of buildings, specially selected accelerograms of real earthquakes, characteristics of earthquake recurrence adopted on the basis of the "Map of seismic zoning of the territory of the Republic of Kazakhstan" are used.

3 RESULTS AND DISCUSSION

At the beginning, the calculations of 10-mass nonlinear systems for 8 real accelerograms of 8- and 9-point earthquakes were performed. The purpose of the calculations was to study the patterns of deformation of the object. And under seismic impact, as well as analysis of the magnitude of the decrease in seismic forces as a result of the use of kinematic foundations. Table 1 shows the indicated accelerograms and their parameters. The frequency composition of accelerograms is very different. In the calculations, segments of accelerograms of 14-16 s were taken.

It was revealed that when exposed to real accelerograms, object A is deformed mainly as a single-mass system, i.e. the deformation of the above-foundational part of the building is small compared to the displacements at the KF level (Fig. 1). Table 2 shows the values of the maximum displacements in the KF level of object A when exposed to accelerograms of different frequency composition and intensity from Table 1.

Table 3 shows the maximum values of distortions and reactions at the level of the 1st residential floor (2nd tier) also obtained when calculating the indicated accelerograms. The values with the reduction of skews K_{Δ} and the response K_R for the building floor data are calculated.

Values K_{Δ} range from 1.83-4.16 and values K_R range from 1.12-2.48. The values of K_{Δ} and K_R differ significantly, which is a consequence of the substantially nonlinear deformation of object A. The mean values of K_{Δ} and K_R for the sample of accelerograms have the corresponding values of 2.76 and 1.9. The indicated values can be taken as a starting point when analyzing the efficiency of KF for buildings of the 158 series. It was revealed that such values of the reaction coefficient lead to a twofold decrease in seismic forces, which corresponds to an increase in the seismic resistance of the building by 1 point.

The displacement values at the KF level, obtained from static and dynamic tests, are 2.4 cm and 1.3 cm, respectively. Comparing them with the calculated KF displacements under the influence of various accelerograms, it is possible to estimate the intensity of the impact created during field tests.

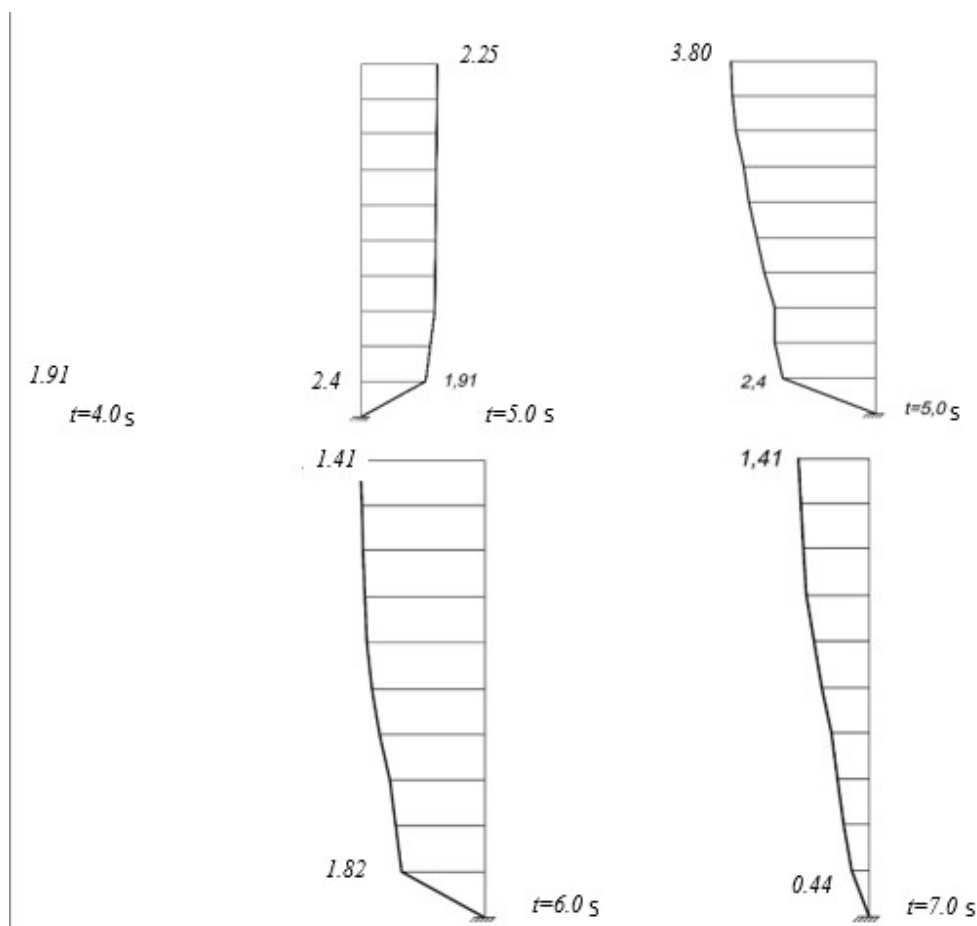


Fig. 1. Deformations of object A at different points in time under the influence of the Sholam Shandon accelerogram 01/27/66.

Since object A was deformed mainly as a single-mass system, it is advisable to use a single-mass design scheme to assess the displacement at the KF level. The weight is taken equal to 27000 kH, and the piecewise linear deformation diagram has the form as in [2]. The value of internal viscous friction is equal to $\mu = 33$. Here the dimension $[\mu] = \text{kN} \cdot \text{s} / \text{cm}$.

Table 1. Parameters of accelerograms of strong earthquakes

No	Place and time of registration	$\ddot{X}_0, \text{cm}/\text{s}^2$	$\sigma, \text{cm}/\text{s}^2$
1	Cholam-Shandon, 27.01.66	342.4	67.16
2	California, 21.07.52	175.9	43.49
3	Eureka, 21.12.54	252.7	51.69
4	Hollister, 08.04.61	175.7	31.05
5	Temblor, 27.06.66	402.8	57.18
6	California, 10.03.33	321.0	58.75
7	El-Centro, 18.05.40	341.7	75.80
8	Cholam-Shandon, 27.01.66	499.0	105.95

Table 2. Movements of object A in the KF level

No, acc.	X_{KF}, cm	
	Multi-mass system	Single-mass system
1	4.27	1.06
2	2.40	2.30
3	4.14	4.65
4	2.26	3.02
5	1.63	2.24
6	4.96	4.13
7	8.40	9.87
8	11.55	11.96

Table 3. Values of reaction coefficients for skews K_{Δ} and reactions K_R

№, acc.	Δ_A , cm	Δ_{KF} , cm	K_{Δ}	R_A , kN	R_{KF} , kN	K_R
1	0.495	0.270	1.83	6944	6222	1.12
2	0.627	0.196	3.20	10817	4676	2.31
3	1.057	0.254	4.16	11819	5978	1.98
4	0.618	0.203	3.04	10719	4574	2.34
5	0.733	0.200	3.67	11838	4772	2.48
6	0.602	0.320	1.88	10763	6863	1.57
7	0.838	0.473	2.11	11383	9037	1.26
8	1.493	0.689	2.17	24165	11162	2.16
average	0.808	0.326	2.75	12306	6660	1.90

Calculations were carried out for the effect of 35 accelerograms of various frequency composition and intensity (Table 4). All accelerograms are divided into groups. Seven-point accelerograms correspond to the acceleration value at the base of 50-120 cm/s², eight-point - 120-240 cm/s², nine-point - 240-500 cm/s². Thus, according to the MSK scale, there are 64 seven-point accelerograms - 7, eight-point - 17, nine-point - 10. One accelerogram corresponds to a ten-point impact (№ 35). Table 5 shows the statistical characteristics (average value and coefficient of variation) of the maximum values of acceleration for the indicated three groups of accelerograms.

Table 4. Reaction of series 158 building on kinematic foundations

№	Accelerogram	max \ddot{y}_0 cm/s ²	Reaction			
			X, cm	\dot{X} , cm/s ²	\ddot{X}_0 , cm/s ²	R_T
1	Eureka, 21.12.54	252.7	4.65	47.50	240.42	6322
2	El-Centro, 18.05.40	341.7	9.87	74.39	377.35	10132
3	Hollister, 08.04.61	175.7	3.02	29.95	194.11	5134
4	California, 21.07.52	175.9	2.30	26.26	171.73	4606
5	San Jose, 04.09.55	105.8	0.52	11.28	108.84	2963
6	El Alamo, 09.02.56	50.1	0.82	10.77	126.63	3447
7	Los Angeles, 09.02.71	398.1	17.61	108.99	585.08	15784
8	Borrego Montano, 08.04.68	127.8	1.21	12.78	140.50	3812
9	California, 1933 г.	321.0	4.13	35.85	222.06	5941
10	San Francisco, 22.03.57	102.8	0.80	12.89	126.16	3428
11	Eureka, 21.12.54	164.5	2.48	29.78	179.20	4738
12	Santa Barbara, 21.07.52	132.2	2.56	24.34	177.79	4791
13	Ferndale, 21.12.54	163.2	6.67	45.89	291.63	7795
14	Golden-Gate, 22.03.57	124.2	0.83	13.38	127.5	3465
15	Olympia, 13.04.49	179.4	3.28	32.11	198.8	5323
16	El-Centro, 30.12.34	395.6	3.92	46.67	221.8	5792
17	Helena, 31.10.35	152.9	1.06	15.46	137.40	3696
18	Helena, 31.10.35	138.2	0.92	13.96	133.20	3591
19	Golden Gate, 22.03.57	103.5	0.50	9.41	203.40	2829
20	Taft, 12.07.1952	173.3	1.93	22.59	163.32	4336
21	El-Centro, 08.04.68	139.4	1.54	14.01	144.12	3909
22	Cholam-Shandon, 27.06.66	342.4	1.06	13.29	136.06	3698
23	Cholam-Shandon, 27.06.66	171.9	2.69	31.72	183.29	4887
24	El-Centro, 30.12.34	165.69	2.65	29.44	182.90	4863
25	San Francisco, 22.03.57	83.8	0.51	9.52	107.69	2924
26	San Francisco, 22.03.57	81.8	0.46	9.05	102.94	2814
27	San Francisco, 22.03.57	82.4	0.35	6.99	92.53	2529
28	Cholam-Shandon, 27.06.66	499.03	11.96	75.81	436.01	11657
29	Eureka, 21.12.54	155.70	6.61	45.57	289.88	7749
30	Los Angeles, 09.02.71	252.80	5.82	50.84	269.99	7171
31	California, 21.07.52	152.7	1.84	21.18	158.01	4265
32	Carpathians, 04.03.77	250.0	13.93	68.80	485.19	13097
33	Hollister, 09.03.49	127.8	2.61	25.64	181.34	4836
34	Temblor, 27.06.66	402.8	2.24	29.20	178.66	4558
35	Gazli, 17.05.76	704.0	14.76	83.81	558.30	13701

Table 5. Statistical characteristics of accelerogram groups

I, b	Average value, cm /s ²	The coefficient of variation
7	87.17	0.22
8	154.15	0.12
9	345.61	0.23

Table 6. Statistical characteristics of the response parameters of the 158 series building with KF, modeled by a single-mass system

Options	7 points		8 points		9 points	
	Sample mean	The coeff. of variation	Sample mean	The coeff. of variation	Sample mean	The coeff. of variation
Displacement, cm	0.566	0.31	2.600	0.65	7.512	0.73
Speed, cm/s	9.987	0.19	25.531	0.40	55.194	0.50
Acceleration, cm/s ²	109.74	0.11	179.69	0.26	315.26	0.47
Reaction, kN	2990	0.11	4811	0.26	8411	0.48

The calculated values of the maximum values of displacement, speed, acceleration and reaction were statistically processed by groups of accelerograms. Table 6 shows the results of statistical analysis. Noteworthy is the nonlinear dependence of the reaction parameters on the intensity of exposure.

Table 2 shows the displacements X_{KF} in the KF level according to the multi-mass and single-mass computational models. The differences in X values for both cases are small.

To predict displacement X_{KF} at the KF level under local influences using the methods of linear regression analysis, a dependence X_{KF} on the magnitude of acceleration at the base was obtained

$$X_{KF} = 0.010755183 \ddot{X}_0 + 3.801877 \quad (1)$$

Where \ddot{X}_0 in cm/s², X_{KF} in cm.

Dependence (1) was obtained from a sample of 10 accelerograms of nine-point earthquakes. Table 7 shows the values X_{KF} calculated by the formula (1) for various values of acceleration at the base \ddot{X}_0 . The first line corresponds to the median value of the earthquake acceleration with a repeatability of 475 years for the city of Almaty, and the second - 2475 years (Map of seismic zoning of the Republic of Kazakhstan).

Table 7. Calculated displacements at the level of the KF support at acceleration values from the Seismic zoning map of the Republic of Kazakhstan

\ddot{X}_0 , cm/s ²	X_{KF} , cm
373	8.08
716	11.50

It is interesting to compare the results obtained with the analysis for a group of nine-point earthquakes (Table 6), where the value $X_{KF} = 7.5$ cm was obtained. For the calculated impact intensity in Table 7 shows the values of 8.08-11.50 cm. A nine-point impact gives an estimate of displacements close to the lower boundary of the specified interval.

It should be noted that here the value of the internal viscous friction parameter significantly affects the reliability of the system. Apparently for the case of high intensity impact, energy dissipation significantly affects the response of the building.

4 CONCLUSIONS

- Kinematic foundations are an effective seismic isolation tool that halves seismic forces, and the floor misalignments by 2.5 times.
- A single-mass design scheme is acceptable for evaluating the response of a seismically isolated house.
- The proposed method for calculating seismically isolated systems can be used to study any kinematic type systems, for example, on rubber blocks [6,14,15].
- When providing movement at the KF level of the order of up to 10-12 cm, the building should be recognized as seismic resistant at the median values of acceleration at the base of the "Map of seismic zoning of the Republic of Kazakhstan" for Almaty.
- The proposed method for accounting for quantitative data on accelerations of the new "Seismic zoning map of the Republic of Kazakhstan" is the second way to take into account the real nature of seismic

impact when calculating seismically isolated systems. Its results do not contradict the results of applying the probabilistic approach [4].

- It should be noted that since December 2019, only the regulatory framework based on Eurocode 8 has been in effect. This regulatory document contains a whole chapter on the design of seismically isolated buildings [18]. The proposed method for predicting displacements at the level of a seismic isolation support can be used to select the optimal parameters of these systems.

5 ACKNOWLEDGMENT

The research was carried out using the funds of the grant AP 05130702 of the Ministry of Education and Science of the Republic of Kazakhstan.

6 REFERENCES

- [1] Cherepinsky, Yu. D., Lapin, V.A. (1995). Fundamentals of Seismic Isolation in Construction. Irkutsk: *ELITE Publishing House*.
- [2] Cherepinsky, Yu. D. (2003). Seismic isolation of residential buildings. Almaty: *KazGASA*.
- [3] Lapin, V.A., Yerzhanov, S.Y., Aldakhov, Y.S. (2020). Special polygon for investigation of seismic insulation properties of foundations. *Journal of Physics: Conference Series*, no. 1614 012009, DOI:10.1088/1742-6596/1614/1/012009
- [4] Lapin, V.A., Yerzhanov, S.Y., Aldakhov, Y.S. (2020). Statistical modeling of a seismic isolation object under random seismic exposure. *Journal Physics: Conference Series*, no. 1425, 1-9, from <http://doi.org/10.1088/1742-6596/1425/1/0112006>.
- [5] Wei Biao, Wang Peng, He Xuhui, Jiang Lizhong. (2018). Seismic Isolation Characteristics of a Friction System. *Journal of Testing & Evaluation*, no. 46 (4), 1-10, DOI:10.1520/JTE20160598
- [6] Bulat, A. F., Dyrda, V. I., Lysytsya, M.I., Grebenyuk, S. M. (2018). Numerical Simulation of the Stress-Strain State of Thin-Layer Rubber-Metal Vibration Absorber Elements Under Nonlinear Deformation. *Strength of Materials*, no. 50(3), 387–395, from <http://doi.org/10.1007/s11223-018-9982-9>
- [7] Giarlelis, C., Kofalis, D., Repapis, C. (2020). Seismic Isolation: An Effective Technique for the Seismic Retrofitting of a Reinforced Concrete Building. *Structural Engineering*, no. 30(1), 43-52, from <http://doi.org/10.1080/10168664.2019.1678449>
- [8] Casablanca, O., Venture, G., Garesci, F., Azzerboni, B., Chiaia, B., Chiappini, M. (2018). Seismic Isolation of building using composite foundation based on metamaterials. *Journal of Applied Physics*, no. 123(17), from <http://doi.org/10.1063/1.5018005>
- [9] Ishii, K., Kikuchi, M. (2019). Improved numerical analysis for ultimate behavior of elastometric seismic isolation bearings. *Earthquake Engineering & Structural Dynamics*, no. 48(1), 65-77, from <http://doi.org/10.1002/eqe.3123>
- [10] Marsis, N. (2019). Seismic isolation: Early history. *Earthquake Engineering & Structural Dynamics*, no. 48(1), 269-283, from <http://doi.org/10.1002/eqe.3124>
- [11] Yerzhanov, S. (2020). On some issues of taking account of the interaction of seismically isolating pile foundations with foundation soil under seismic effects. *16th World Conference on Seismic Isolation, Energy Dissipation on Active Vibration Conference of Structures*, 955-963, from <http://doi.org/10.13753./2686-7974-2019-16-919-927>
- [12] Lapin, V. (2020). Comparative Analysis of the Effect of Seismic Isolation by Means of Stations of Engineering Seismometric Service on Buildings. *16th World Conference on Seismic Isolation, Energy Dissipation on Active Vibration Conference of Structures*, 325-332, from <http://doi.org/10.13753./2686-7974-2019-16-482-527>
- [13] Tsang, H., Pitiliakis, K. (2019). Mechanism of geotechnical seismic isolation system: Analytical modeling. *Soil Dynamics & Earthquake Engineering*, no. 122, DOI:10.1016/j.solidyn.2019.03.37
- [14] Bulat, A.F., Dyrda, V.I., Grebenyuk, S.N., Agal'tsov, G. N. (2019). Methods for evaluating the characteristics of the stress-strain state of seismic blocks under operating conditions. *Strength of Materials*, no. 51(5), 715-720, from <https://doi.org/10.1007/s11223-019-00129-x>
- [15] Bulat, A.F., Dyrda, V.I., Grebenyuk, S.N., Klimenko, M.I. (2019). Determination of effective characteristics of the fibrous viscoelastic composite with transversal and isotropic components. *Strength of Materials*, no. 51(2), 183-192, from <https://doi.org/10.1007/s11223-019-00064-x>
- [16] Smirnov, V.I. (2009). Testing of buildings with seismic isolation systems with dynamic loads and real earthquakes. *Earthquake-resistant construction. Safety of structures*, no. 4, 16-22.
- [17] Mikhailova, N.N., Uzbekov, A.N. (2018). Tectonic and technogenic earthquakes in central Kazakhstan. News of the national academy of sciences of the republic of Kazakhstan. *Series of geology and technical sciences*, no. 429(3), 146-155.

- [18] Fardis, M., Carvalho, O., Elnashai, A., Faccioli, E., Pinto, P., Plumier, A. (2013). Designer's Guide to Eurocode 8: Design of earthquake-resistant structures: General design standards for earthquake-resistant structures, seismic effects, building and retaining structure design rules. Moscow: MGSU.

Paper submitted: 23.12.2021.

Paper accepted: 06.07.2022.

This is an open access article distributed under the CC BY 4.0 terms and conditions.